(D)

AD

TECHNICAL REPORT ARBRL-TR-02406

MULTIPLE IMPACTS ON MONOLITHIC STEEL

V. Kucher

April 1982

US ARMY ARMAMENT RESEARCH AND DEVELOPMENT COMMAND
BALLISTIC RESEARCH LABORATORY
ABERDEEN PROVING GROUND, MARYLAND

Destroy this report when it is no longer needed. Do not return it to the originator.

Secondary distribution of this report by originating or sponsoring activity is prohibited.

Additional copies of this report may be obtained from the National Technical Information Service, U.S. Department of Commerce, Springfield, Virginia 22161.

The findings in this report are not to be construed as an official Department of the Army position, unless so designated by other authorized documents.

The use of trade names or manufacturers' names in this report does not constitute indorsement of any commercial product.

UNCLASSIFIED

SECURITY CLASSIFICATION OF THIS PAGE (When Data Entered)

REPORT DOCUMENTATION PAGE		READ INSTRUCTIONS BEFORE COMPLETING FORM
1. REPORT NUMBER Technical Report ARBRL-TR-02406	2. GOVT ACCESSION NO. AD-A114 038	3. RECIPIENT'S CATALOG NUMBER
4. TITLE (and Subtitle) MULTIPLE IMPACTS ON MONOLITHIC STEEL		5. TYPE OF REPORT & PERIOD COVERED FINAL 6. PERFORMING ORG. REPORT NUMBER
7. AUTHOR(s) V. Kucher		8. CONTRACT OR GRANT NUMBER(s)
9. PERFORMING ORGANIZATION NAME AND ADDRESS US Army Ballistic Research Laboratory (ATTN: DRDAR-BLT) Aberdeen Proving Ground, MD 21005		10. PROGRAM ELEMENT, PROJECT, TASK AREA & WORK UNIT NUMBERS 1L161102AH43
11. CONTROLLING OFFICE NAME AND ADDRESS US Army Armament Research and Development Command US Army Ballistic Research Laboratory (DRDAR-BL) Aberdeen Proving Ground, MD. 21005		12. REPORT DATE April 1982 13. NUMBER OF PAGES 43
14. MONITORING AGENCY NAME & ADDRESS(if different from Controlling Office)		15. SECURITY CLASS. (of this report) UNCLASSIFIED 15a. DECLASSIFICATION/DOWNGRADING SCHEDULE

16. DISTRIBUTION STATEMENT (of this Report)

Approved for public release; distribution unlimited.

17. DISTRIBUTION STATEMENT (of the abstract entered in Block 20, if different from Report)

18. SUPPLEMENTARY NOTES

19. KEY WORDS (Continue on reverse side if necessary and identify by block number)

Penetration mechanics
Two-dimensional computer code
Eulerian computer code
Shaped-charge penetration
Multiple impact

20. ABSTRACT (Continue on reverse side if necessary and identify by block number)

The multiple impacts on a monolithic, semi-infinite steel target of a shaped-charge jet in a particulated state were computer simulated by right circular cylinders, having a diameter of 3 mm and moving initially at 5 km/s. The penetration histories of two and six penetrators at separation distances of 0, 10, and 50 mm were computed using the DORF code. In each case, the combined length of the penetrators was 27 mm, thereby, preserving the initial total momentum and total kinetic energy of the system. The effects of the number of penetrators and the distance between the penetrators on the total penetration

DD FORM 1 JAN 73 1473 EDITION OF 1 NOV 65 IS OBSOLETE

UNCLASSIFIED

SECURITY CLASSIFICATION OF THIS PAGE (When Data Entered)

and final hole profile were determined.

TABLE OF CONTENTS

LIST OF ILLUSTRATIONS

LIST OF ILLUSTRATIONS

I. INTRODUCTION

When a shaped-charge jet is formed, it is, in its early stages, a continuous, constantly stretching jet of liner material. Eventually, the jet breaks up into particulates with different velocities and with various distances between particulates. These distances between the particulates increase with increasing standoff distance of the shaped charge from the target. Furthermore, as the standoff distance increases, the time of flight increases, and the particulates can start to tumble. This tumbling can cause the particulates to deviate from a straight path[1] and thereby reduce the penetration efficiency of the shaped charge.

The maximum depth of penetration occurs when the particulates are axially aligned along a straight path. Then the problem is axisymmetric and can be modeled as a two-dimensional problem. This study deals with this problem of maximum penetration depth and corresponds to the case of an ideally fabricated shaped charge fired against a monolithic target. Although this is the upper limit of penetration, it should provide insight into the penetration phenomena associated with particulated jets[2].

In addition to standoff effects, some of the factors which affect the penetration by particulates are liner and target materials and the diameter and length of each particulate[3,4].

The results of a computer study of the multiple impacts of right cylindrical penetrators, simulating particulates, on a target are reported here. Copper and steel were used, respectively, as penetrator and target materials. Also the diameter and initial velocity of the penetrators were fixed at 3 mm and 5 km/s, respectively. Two situations, where the total mass and the total kinetic energy of all the penetrators before impact were fixed, were examined: (1) the number of penetrators was varied and (2) the distance between the penetrators was varied to simulate different standoff distances. Of interest were the penetration histories of the penetrators and the material flow during penetration.

---

[1] *R. DiPersio, J. Simon, and A. Merendino, "Penetration of Shaped-Charge Jets into Metallic Targets," Ballistic Research Laboratory Report No. 1296, September 1965. (AD 476717)*

[2] *A. Merendino and R. Vitali, "The Penetration of Shaped-Charge Jets into Steel and Aluminum Targets of Various Strengths," Ballistic Research Laboratory Memorandum Report No. 1932, August 1968. (AD 392672)*

[3] *W. P. Walters and J. N. Majerus, "Impact Models for Penetration and Hole Growth," BRL Technical Report ARBRL-TR-02069, May 1978. (AD A056294)*

[4] *W. P. Walters and J. N. Majerus, "Shaped Charge Penetration Model, Part 1: Monolithic Penetration and Comparison with Experimental Data," BRL Technical Report ARBRL-TR-02184, August 1979. (AD B041747L)*

II. COMPUTER PROGRAM

The DORF computer program[5] was used to generate data for this impact phenomena study. DORF is a two-dimensional, multimaterial, continuous, Eulerian, hydrodynamic program coupled with an elastic-plastic strength model. An option of Cartesian (x,y) or cylindrical (r,z) coordinates is available in the program. The later option was selected for this study because of the cylindrical symmetry associated with the impacts. Tillotson's equations of state[6] for copper and steel were used by the program. Tracer particles, whose motion depends upon an average of local cell velocities, were used to provide a Lagrangian appearance to the plotted output of material deformation. The program was run on the CDC CYBER 76 located at ARRADCOM Ballistic Research Laboratory.

III. PENETRATOR-TARGET CONFIGURATIONS

In all the cases that were run on the computer, the impacts were normal (zero obliquity), thus permitting the problem to be considered as being axisymmetric. The penetrator material was copper with a yield stress in shear of 1.3 kbar. Before impact, the velocity of the penetrators was 5.0 km/s and the diameter, 3 mm. The steel target was semi-infinite with a yield stress in shear of 6.8 kbar.

Five impact situations were considered: (1) one impact by a 27.0-mm-long penetrator, (2) two impacts by 13.5-mm-long penetrators separated by 10 mm, (3) two impacts by 13.5-mm-long penetrators separated by 50 mm, (4) six impacts by 4.5-mm-long penetrators separated by 10 mm, and (5) six impacts with 4.5-mm-long penetrators separated by 50 mm.

The initial total mass, total kinetic energy, and total momentum of one 27.0-mm-long penetrator, two 13.5-mm-long penetrators, or six 4.5-mm-long penetrators were, respectively, the same.

IV. COMPUTATIONAL SETUP

A computational grid was laid out to cover the cross-sectional region of interest of the penetrator-target configuration with the penetrator's center line coinciding with the z-axis. A typical configuration is shown in Figure 1. The penetrator's initial motion was in the positive z-direction. The computer program permits an option of

---

[5] *W. E. Johnson, "Development and Application of Computer Programs Related to Hypervelocity Impact," Systems, Science and Software, 3SR-749, July 1971. (AD 889143)*

[6] *J. H. Tillotson, "Metallic Equations of State for Hypervelocity Impact," Gulf General Atomic, GA-3216, July 1962.*

reflective or transmittive boundaries. The bottom boundary of the grid was selected to be transmittive, thus allowing penetrator material to be fed into the grid when the situation so required. The right boundary of the grid was selected to be transmittive, thereby simulating a semi-infinite target. To permit material to flow out of the region of interest and to simulate a semi-infinite target, the top boundary was also transmittive. DORF automatically selects the proper boundary conditions for the left boundary when this boundary is an axis of symmetry.

Typical overall physical dimensions of the grid were 25 mm by 95 mm with a corresponding grid size of 83 by 186 cells. The width, Δr, in the radial direction of each cell was 0.3 mm, except for the rightmost cells which were 0.4-mm wide. Thus the radius of the penetrators was 5 cells across[7]. The length, Δz, of each cell was 0.5 mm, except for the bottom cells which were 2.5-mm long.

If the penetration exceeded the limits of the grid, additional 0.5-mm-long cells were added to the top of the grid.

The cells, occupying the initial space of the penetrators, were given the following initial conditions:

1. Density = 8.9 Mg/m^3.
2. Pressure = 0.0 Mbar.
3. Radial velocity = 0.0 km/s.
4. Axial velocity = 5.0 km/s.
5. Specific internal energy = 0.0 J/g.

Similar initial conditions were given to the cells occupying the initial space of the target except that the density was that of the steel target material, 7.86 Mg/m^3 , and the axial velocity was zero.

In all the cases that were run on the computer, the impact surface of the target was at z = 30 mm on the grid. Tracer particles were positioned along this surface, and, when their positions were line-plotted, the deformation of this surface could be pictured.

Tracer particles were also positioned along the free surfaces of each penetrator. When these positions were line-plotted, the deformation of the penetrators could also be pictured. In addition, tracer particles were positioned within the outline of the penetrators. These positions were point-plotted with different symbols representing different penetrators.

---

[7] *V. Kucher, "Preliminary Computer Computations for Slender Rod Impact Problems," Ballistic Research Laboratory Report No. 1957, Feb 1977. (AD A036995)*

V. COMPUTER RESULTS

A. Single Impact

A copper penetrator, 3.0 mm in diameter and 27.0-mm long, impacted at 5.0 km/s, on a steel target at zero-degrees obliquity. Figure 2 shows the initial penetrator-target configuration, and Figure 3 shows the penetrator-target deformation at 4.0 μs. A corresponding velocity field is shown in Figure 4. Note that there is a flow of material (ejecta) opposite to the original direction of the penetrator.

The trajectories of two tracer particles, which were initially positioned at each end of the penetrator along the axis of symmetry, are shown in Figure 5. At any instant of time, the measured difference between the curves is the length of the material remaining at that time.

The maximum penetration of 38.5 mm, as measured from the initial free surface of the target, occured at 23.9 μs after impact. Figure 6 shows the hole profile at 24.0 μs.

B. Double Impact at Short Standoff

Two copper penetrators, each being 3.0 mm in diameter and each being 13.5-mm long, impacted a steel target at zero-degrees obliquity. Each penetrator initially had a velocity of 5.0 km/s; a distance of 10 mm separated the penetrators.

Figure 7 shows the initial configuration of the target and penetrators. Note that different plotting symbols were used for each penetrator. Figure 8, at 3.0 μs, shows the deformation of the first penetrator after penetrating the target for this period of time. Figure 9 shows the velocity field at 3.0 μs with some of the flow of material in opposition to the initial motion of the penetrators. At 6.0 μs in Figure 10, part of the second penetrator has been deformed by this flow.

The trajectories of the four tracer particles, which were initially positioned at each end of the penetrators along the axis of symmetry, are shown in Figure 11. At any instant of time, the measured difference between the front and back curves is the length of the penetrator remaining at this time. The maximum penetration, 40.8 mm, occurred at 23.0 μs. Figure 12 shows the hole profile at 24.0 μs.

C. Double Impacts at Long Standoff

The initial conditions here are similar to those for the double impact, short standoff situation except that the distance between the penetrators was increased to 50 mm (thus a longer standoff was considered than in the previous case).

In Figure 13, the first penetrator has been consumed, and the flow

of the ejecta out of the cavity in the target has caused some deformation of the front of the second penetrator. The velocity field at 20.0 μs (Figure 14) illustrates the complexity of the material flow. At 22.0 μs (Figure 15), the second penetrator is still acting on the target; an occlusion of target material at z = 48 mm has formed.

The trajectories of the tracer particles, positioned as described in the previous case, are shown in Figure 16. At 16 μs, the penetration due to the first penetrator has almost ceased at about 22 mm of penetration. Now the second penetrator, acting on the target, penetrates the target to a depth of 55 mm at 37.6 μs. A hole profile at 38 μs is shown in Figure 17.

D. Sextuple Impacts at Short Standoff

Six copper penetrators, 3.0 mm in diameter and each being 4.5-mm long, impacted a steel target at zero-degrees obliquity. Each penetrator initially had a velocity of 5 km/s; a distance of 10 mm initially separated the penetrators.

Figure 18 shows the penetration by the first penetrator after 1.0 μs. The second and third penetrators are also pictured with distinguishing symbol plots. At 9.0 μs (Figure 19) the first and second penetrators have been consumed and the third penetrator, which has deformed on the front end, is ready to begin its penetration action. The remaining three penetrators are also shown at this time. The nature of the material flow at 10.0 μs is illustrated by a velocity field in Figure 20.

Trajectories of the tracer particles that were located initially on the front and back surfaces and on the axis of the penetrators are shown in Figure 21. The maximum penetration of 71.6 mm occurred at 39.4 μs. Figure 22 shows the hole profile at 40.0 μs.

E. Sextuple Impacts at Long Standoff

In this case, the initial conditions were similar to those for the sextuple impacts, short standoff case described in the previous case except that the distance between penetrators was increased to 50 mm, thus providing a longer standoff.

Shown in Figure 23 are the trajectories of the tracer particles that were initially located along the axis of symmetry at the front and back surfaces of the penetrators. The maximum penetration of 101.3 mm occurred at 87.0 μs. The hole profile at 88.0 μs is shown in Figure 24.

VI. DISCUSSION

The graphical computer results show that a complex flow of material in the crater, as it is being formed, is created after the impact of the first penetrator and by the succeeding penetrators (Figures 4, 9, and 14). This flow of material in the opposite direction of the motion of the penetrators causes some deformation or erosion of the succeeding penetrators (Figures 10, 13, and 19). Also, as a result of multiple impacts, occlusion of the crater occurs (Figures 15 and 24). However, these phenomena did not, for the initial impact velocity, the number of penetrators, and the separation distances that were considered, decrease the maximum penetration of several penetrators compared to a single penetrator. Figure 25 shows the effects on the maximum penetration of the number of penetrators and their separation distance. The single 27.0-mm-long penetrator can be considered as two 13.5-mm-long penetrators or six 4.5-mm-long penetrators with no separation distance.

Comparing the maximum penetration of two penetrators, we find that there is a 6.0% increase for a 10-mm separation distance and a 42.9% increase for a 50-mm separation distance with respect to the case where there is no separation between the penetrators.

Comparing the maximum penetration of six penetrators with the single penetrator (six penetrators with no separation distance), we find that at a separation distance of 10 mm, there is a 86.0% increase in the maximum penetration and a 163.1% increase in maximum penetration when the separation distance is increased to 50 mm.

When the separation distance for two penetrators is increased from 10 to 50 mm, the maximum penetration increased by 75.5%. Similarly, for six penetrators, the maximum penetration increased by 84.2% when the separation distance was changed from 10 to 50 mm.

Figures 6, 12, 17, 23, and 24, which depict the hole profiles in the target at approximately the time of maximum penetration, show that the eyeball-average diameter of the hole decreases as the length of the penetrator decreases. For the single impact case (27.0-mm-long penetrator) the average hole diameter was 15.0 mm; for the double impact cases (13.5-mm-long penetrators) the average diameter was 13.2 mm; for the sextuple impact cases (4.5-mm-long penetrators) the average diameter was 9.0 mm.

The hole volume table summarizes the volumes calculated from hole profile measurements. The hole volume, which was measured from the original free surface of the target, was 5375.5 mm^3 for the single impact case. This volume was decreased by 1.6% and 21.5%, respectively, for the double and sextuple impact cases at a separation distance of 10 mm. The single impact volume was increased by 42.5% and 66.8%, respectively, for the double and sextuple impact cases with a 50-mm separation distance.

Hole Volumes Resulting from Multiple Impacts

Hole Volume, mm^3

Separation Distance, mm / Number of Penetrators	0	10	50
2	5375.5	5291.6	7662.3
6	5375.5	4219.1	8963.8

For the double impact cases, the hole volume increased 44.8% when the separation distance was changed from 10 to 50 mm. For the sextuple impact cases, the hole volume was increased 112.5% when the separation distance was similarly changed.

For a 10-mm separation distance, the hole volume decreased 20.3% when the number of penetrators was increased from 2 to 6. For a 50-mm separation distance, the hole volume increased 17.0% when the number of penetrators was similarly increased.

VII. CONCLUSIONS

The effects of multiple impacts were considered for a single impact velocity (5 km/s), a fixed total mass of the penetrators, penetrator separation distances of 0, 10, and 50 mm, and single, double, and sextuple impacts. For these conditions, it was found that increasing the number of penetrators and increasing the separation distance between penetrators increased the penetration into a steel target.

Increasing the number of penetrators resulted in the decrease in the average hole diameter in the target. Compared to the single impact case, the hole volume, at the time that the maximum penetration occurred, decreased for the double and sextuple impact cases for 10-mm separation between penetrators, but increased for the 50-mm separation distance.

Increasing the number of penetrators from 2 to 6 for the 10-mm separation decreased the hole volume, but, for the 50-mm separation case, the volume increased.

The results obtained from these computer computations might not follow for other target material or thicknesses, other penetrator velocity ranges, or non-aligned penetrators. Further studies are necessary to investigate these parameters with relation to multiple impacts.

ACKNOWLEDGMENT

Gratitude is expressed to Dr. John Majerus for suggesting this study.

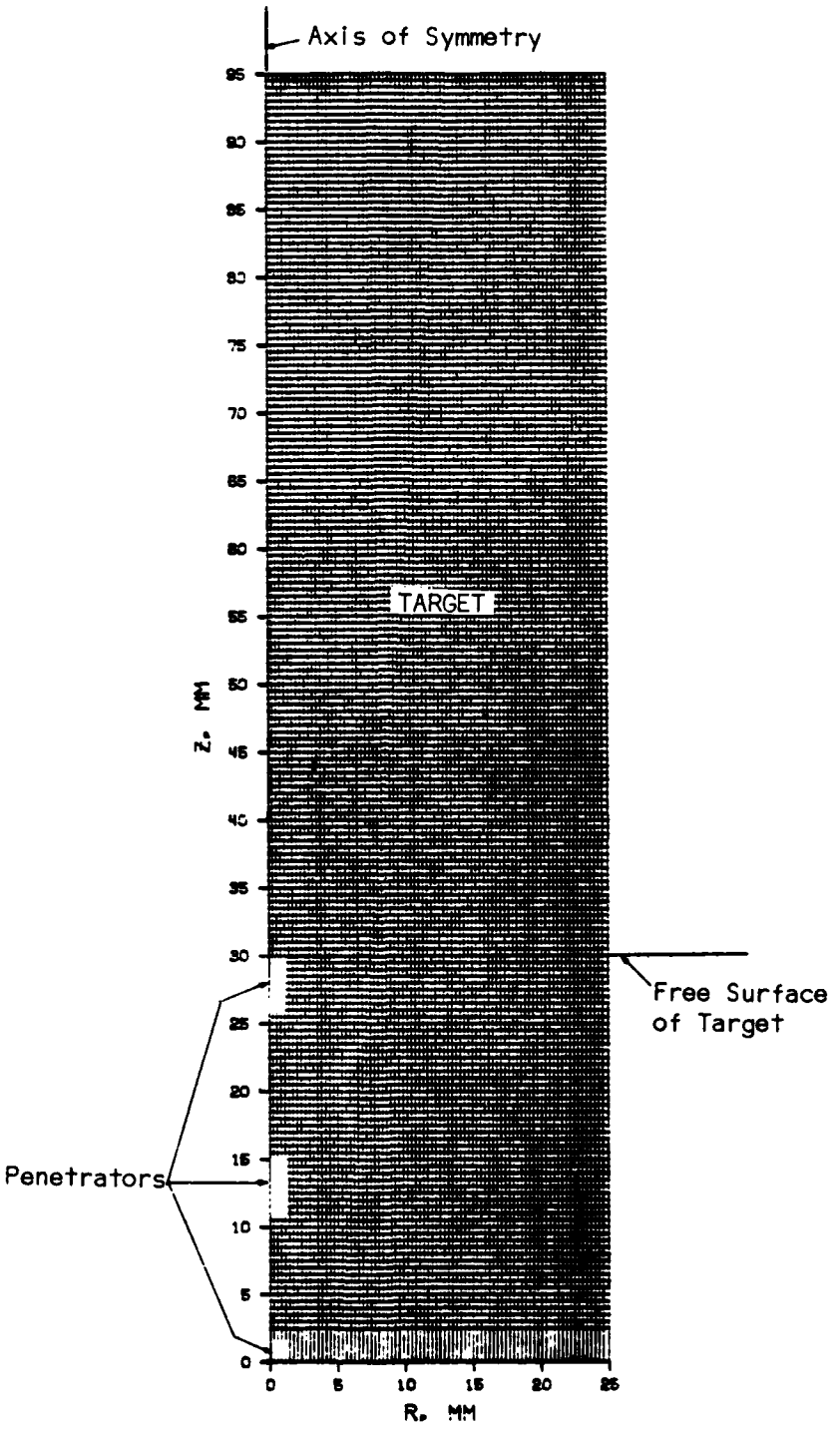

Figure 1. Typical Computational Grid Setup

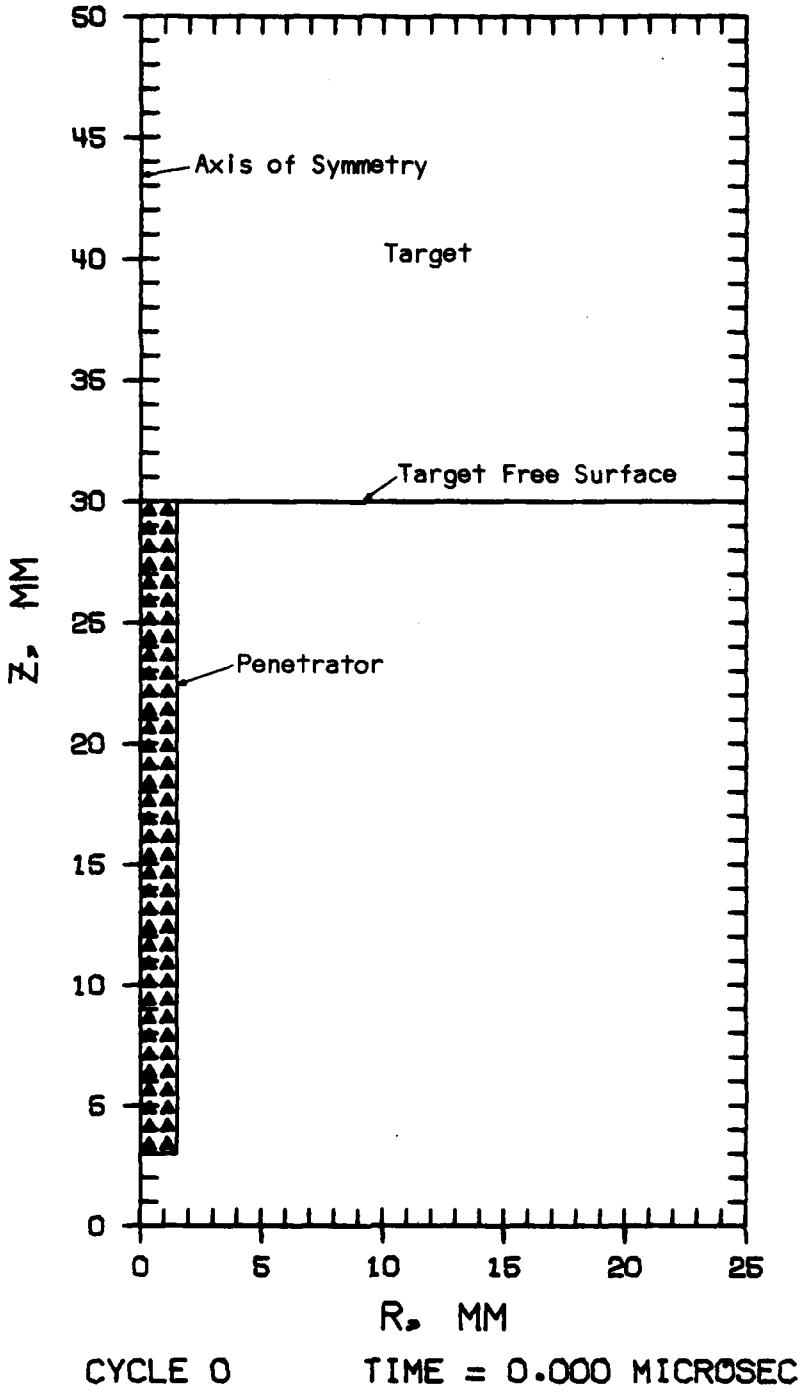

Figure 2. Single Impact Penetrator-Target Configuration

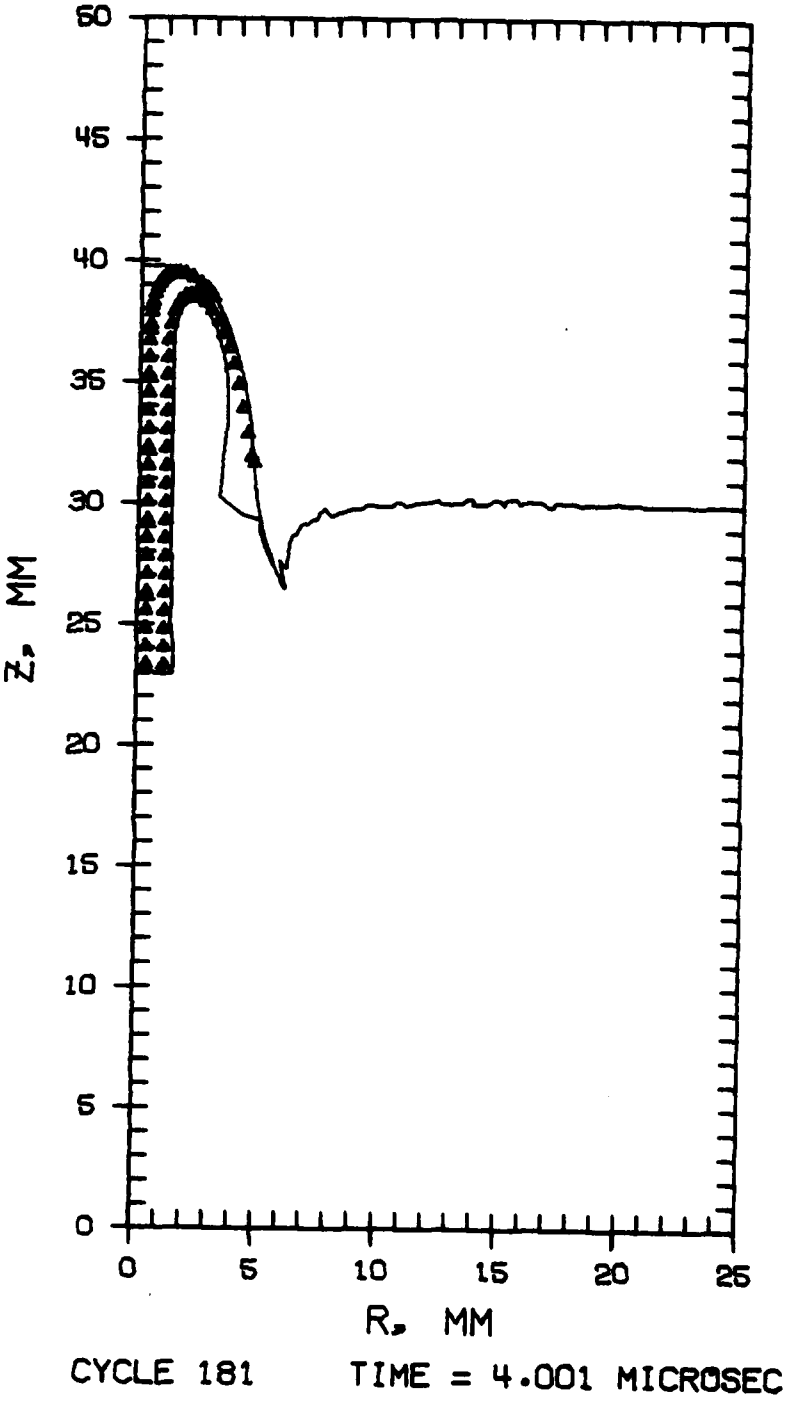

Figure 3. Single Impact Penetrator-Target Deformation

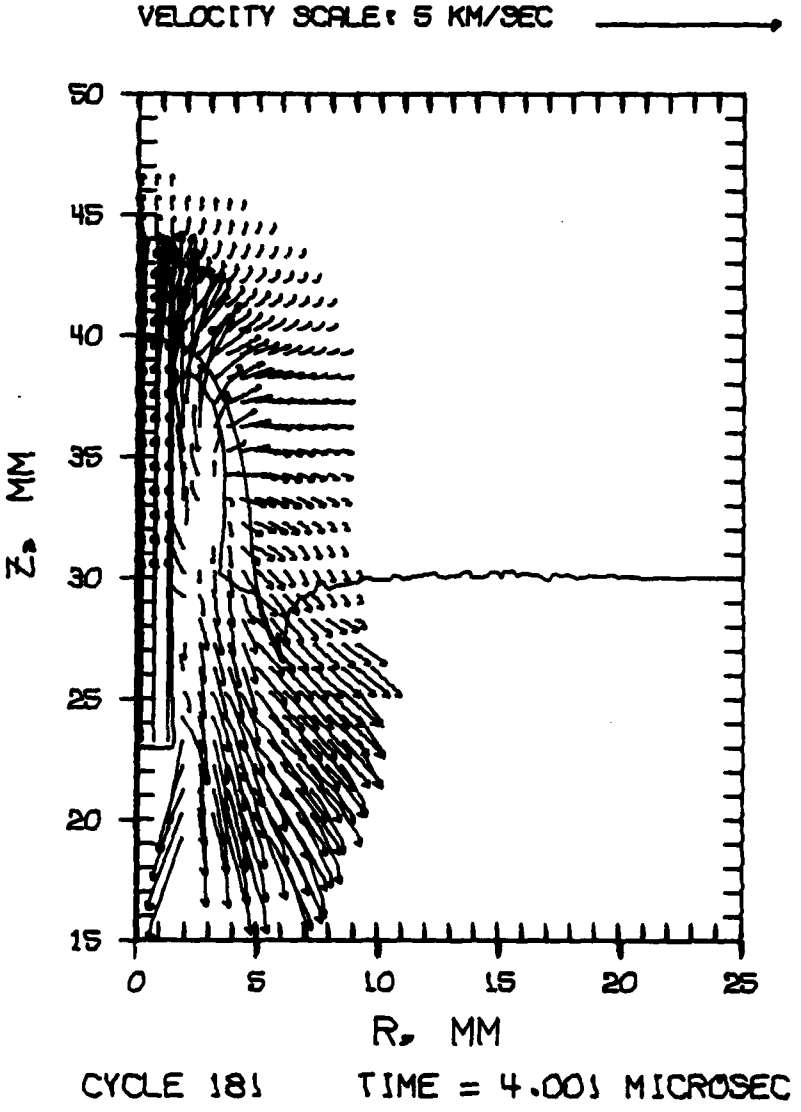

Figure 4. Single Impact Velocity Field

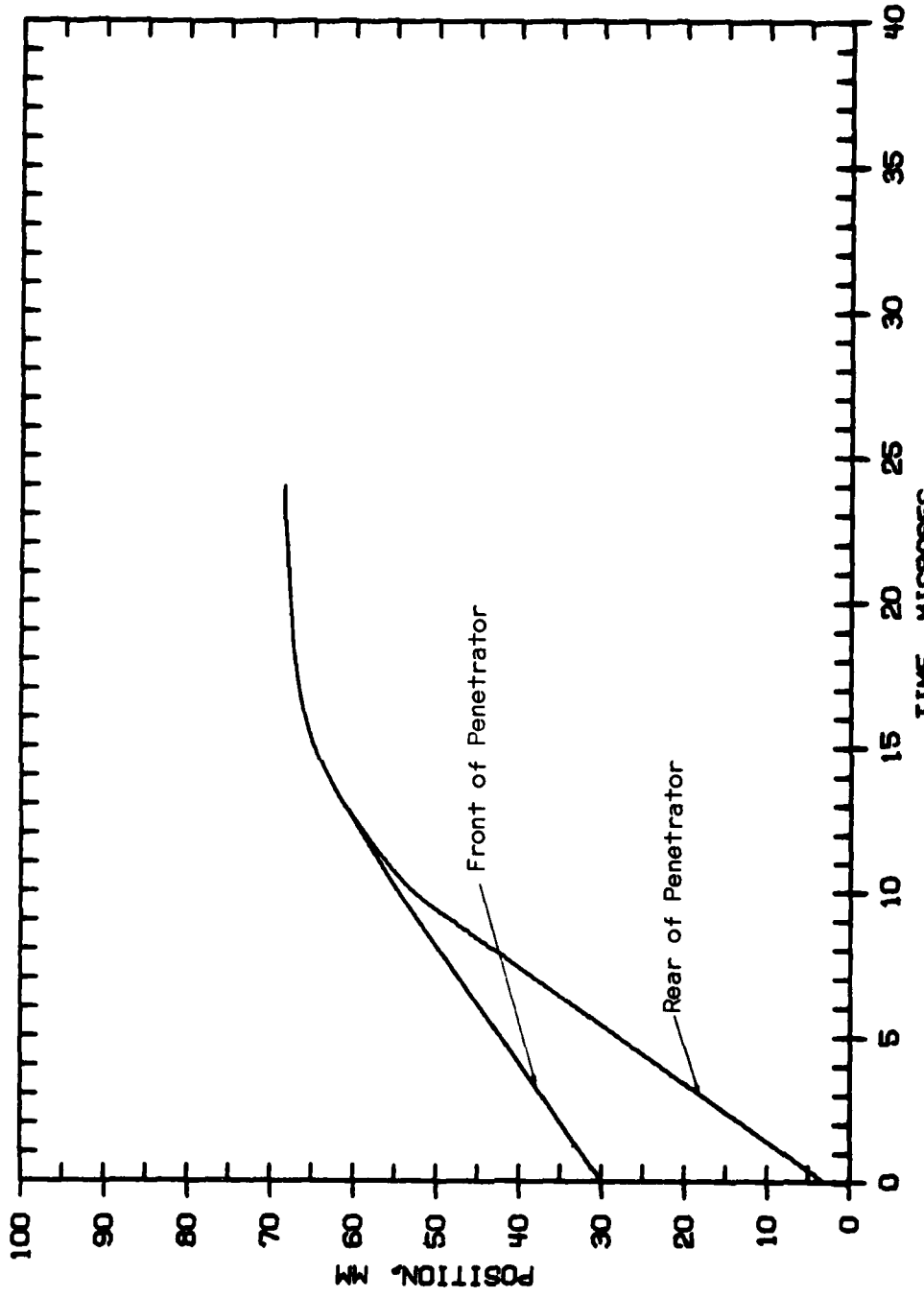

Figure 5. Single Impact Tracer Motion History

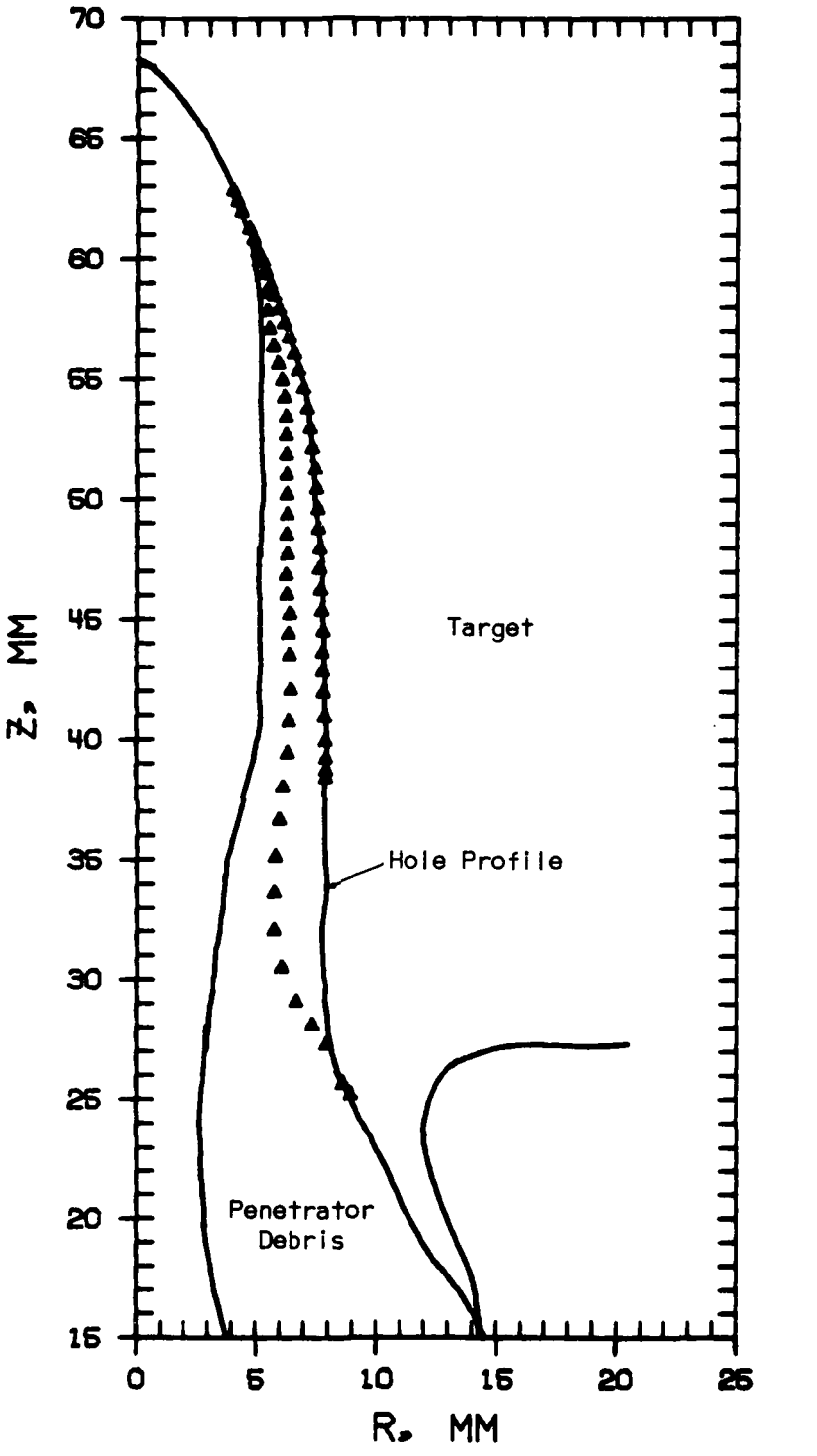

Figure 6. Single Impact Hole Profile

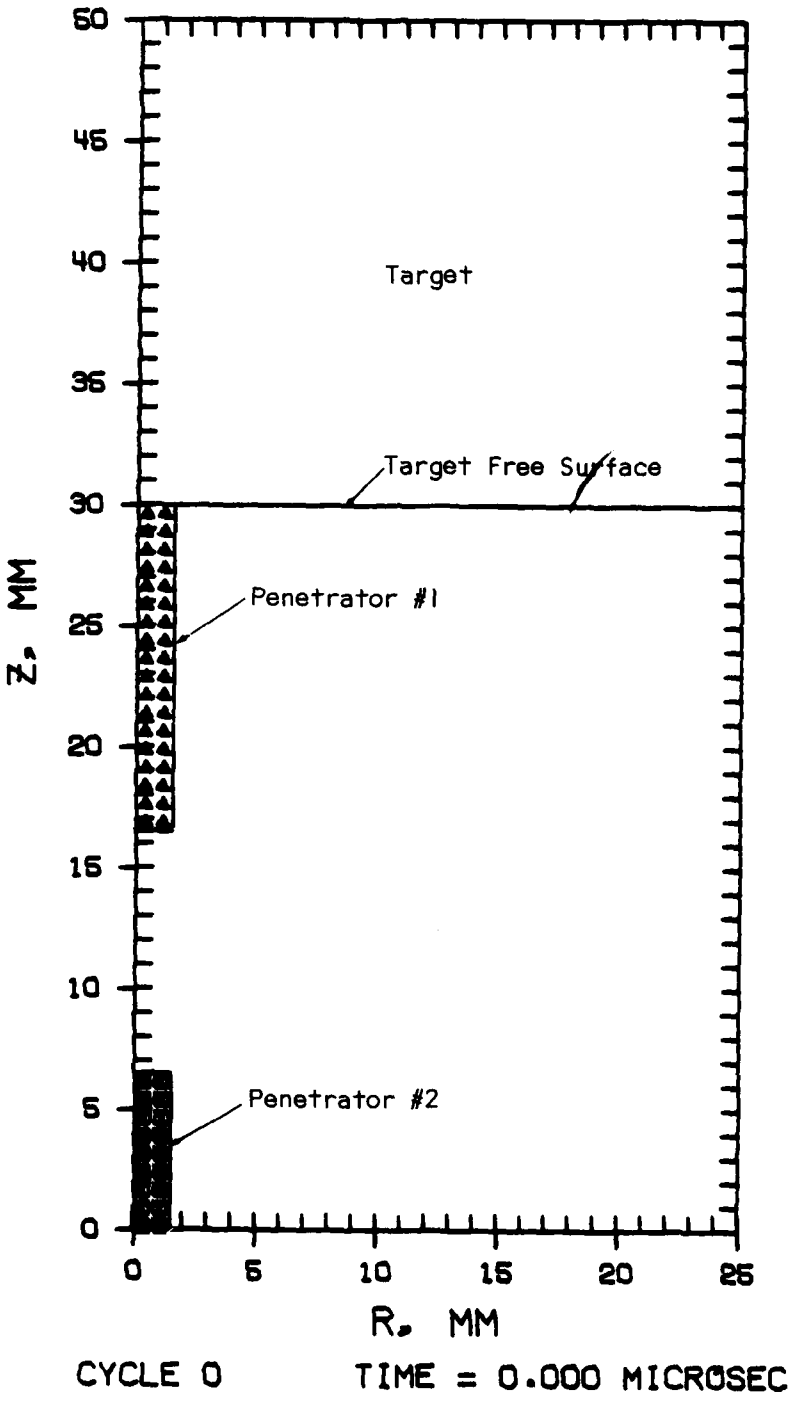

Figure 7. Double Impact Penetrator-Target Configuration for a 10-mm Penetrator Separation

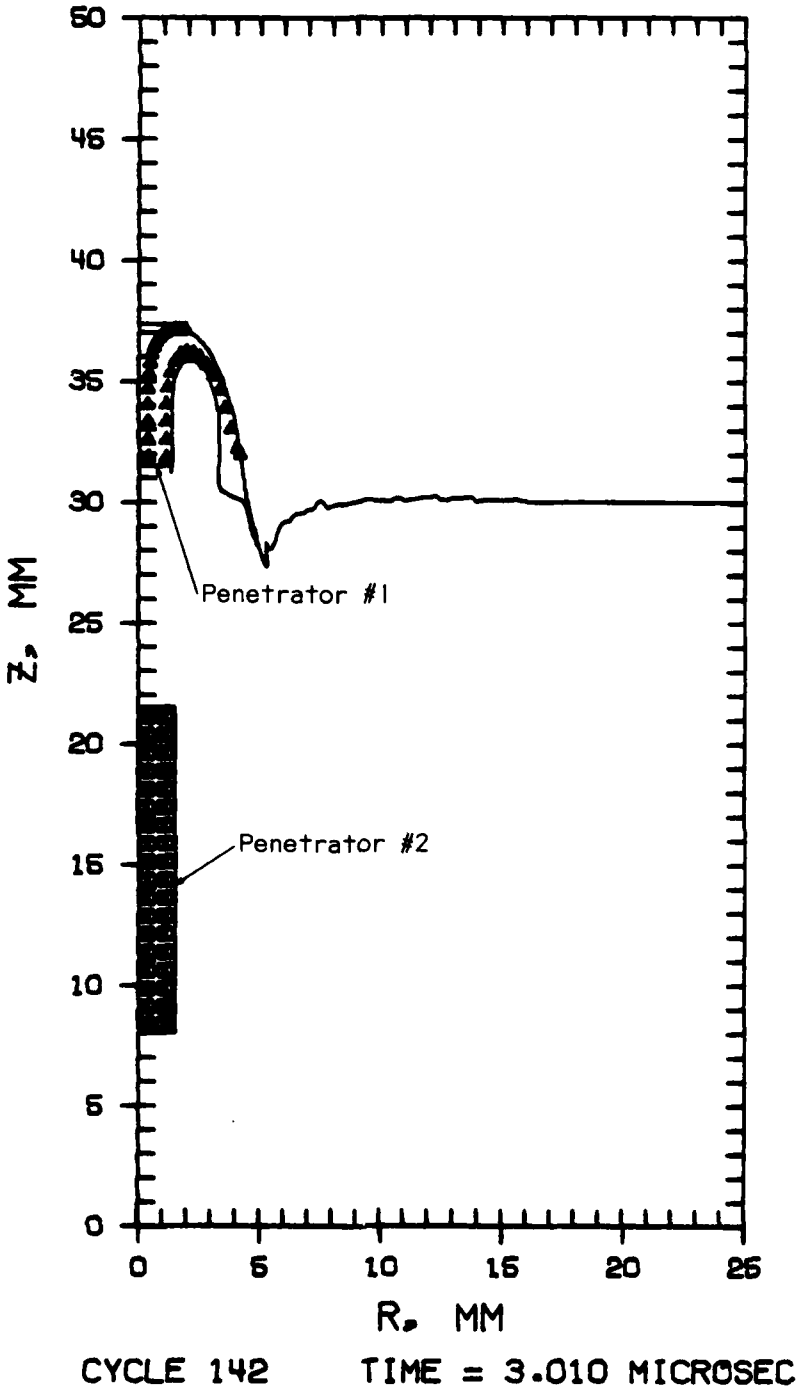

Figure 8. Double Impact Penetrator-Target Deformation for a 10-mm Penetrator Separation

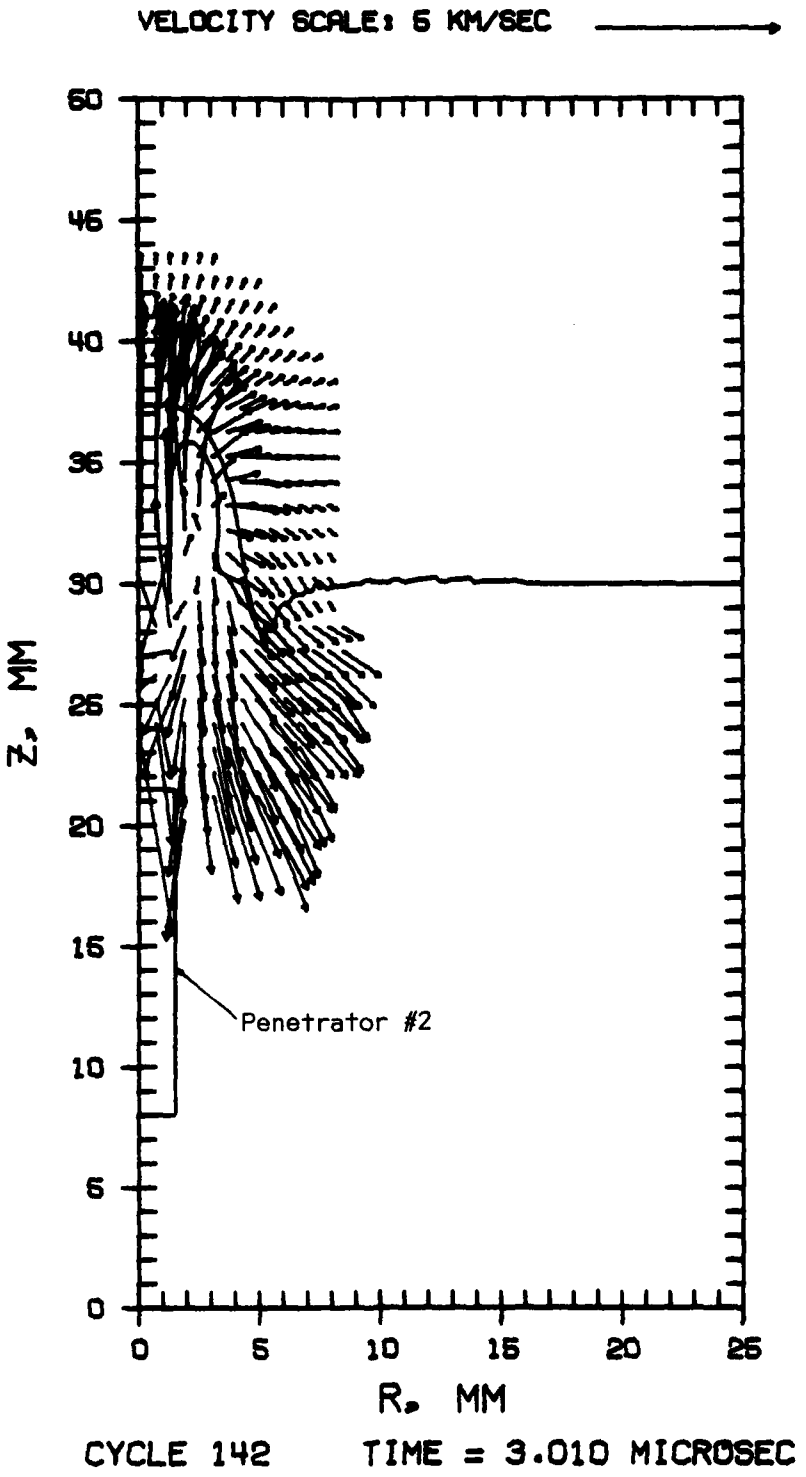

Figure 9. Double Impact Velocity Field for a 10-mm Penetrator Separation

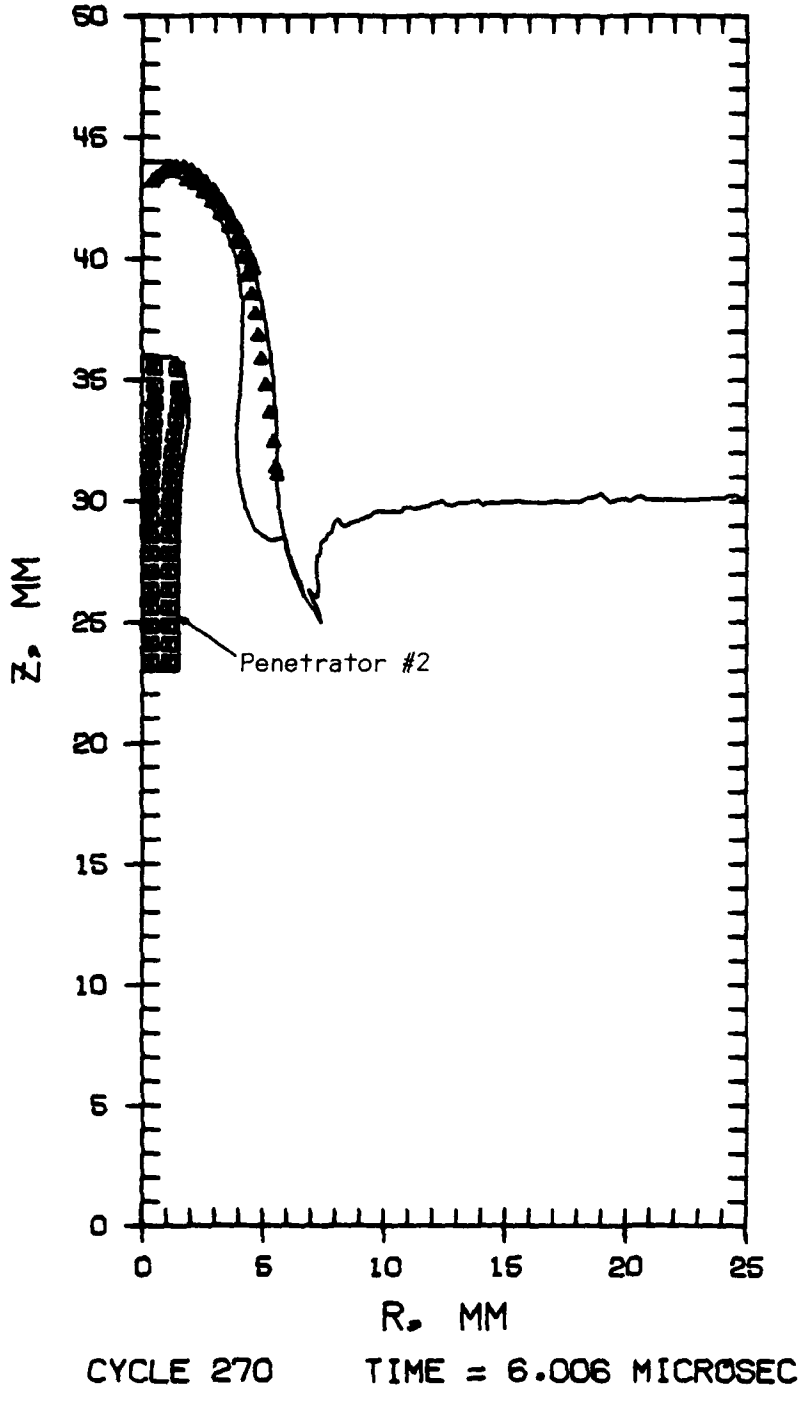

Figure 10. Double Impact Penetrator-Target Deformation for a 10-mm Penetrator Separation

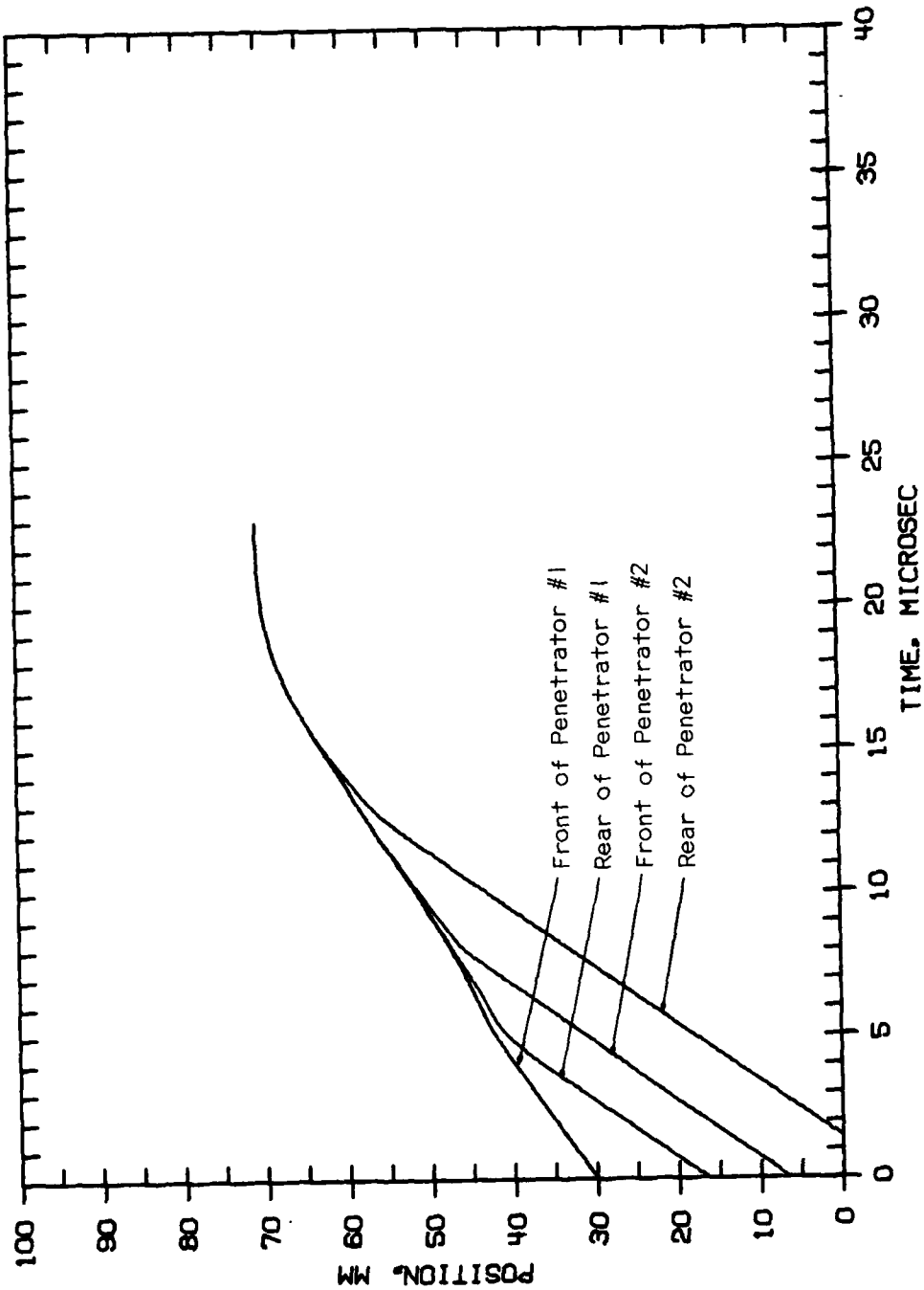

Figure 11. Double Impact Tracer Motion History for a 10-mm Penetrator Separation

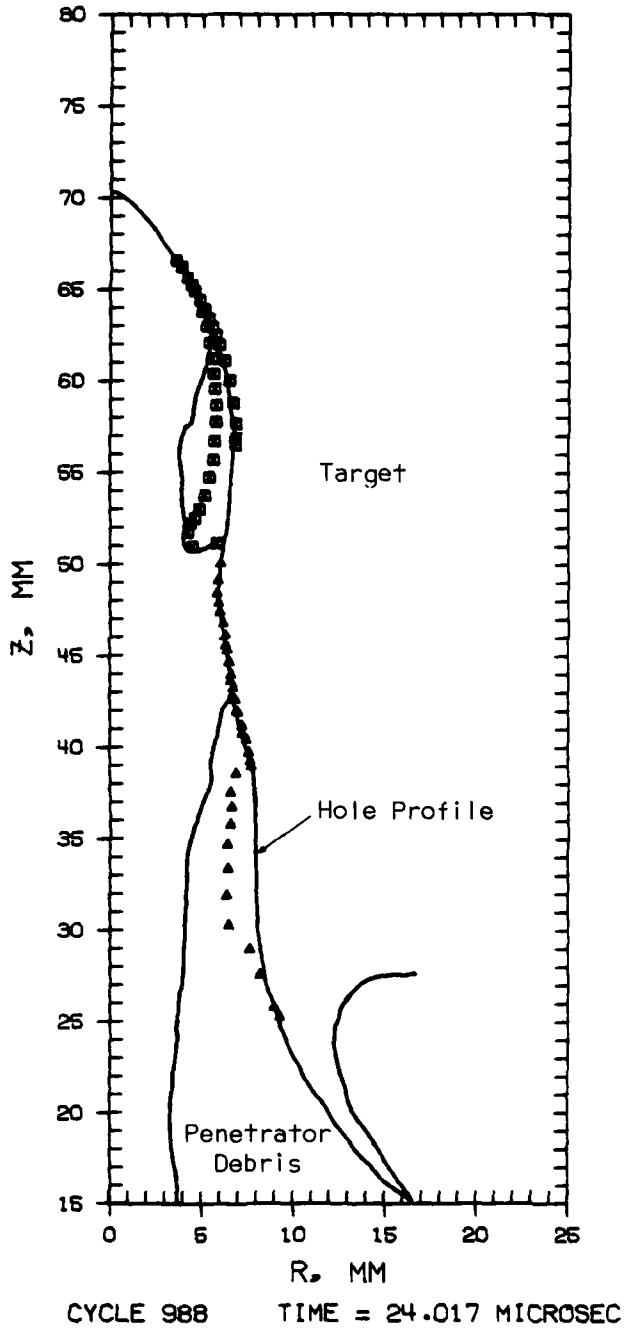

Figure 12. Double Impact Hole Profile for a 10-mm Penetrator Separation

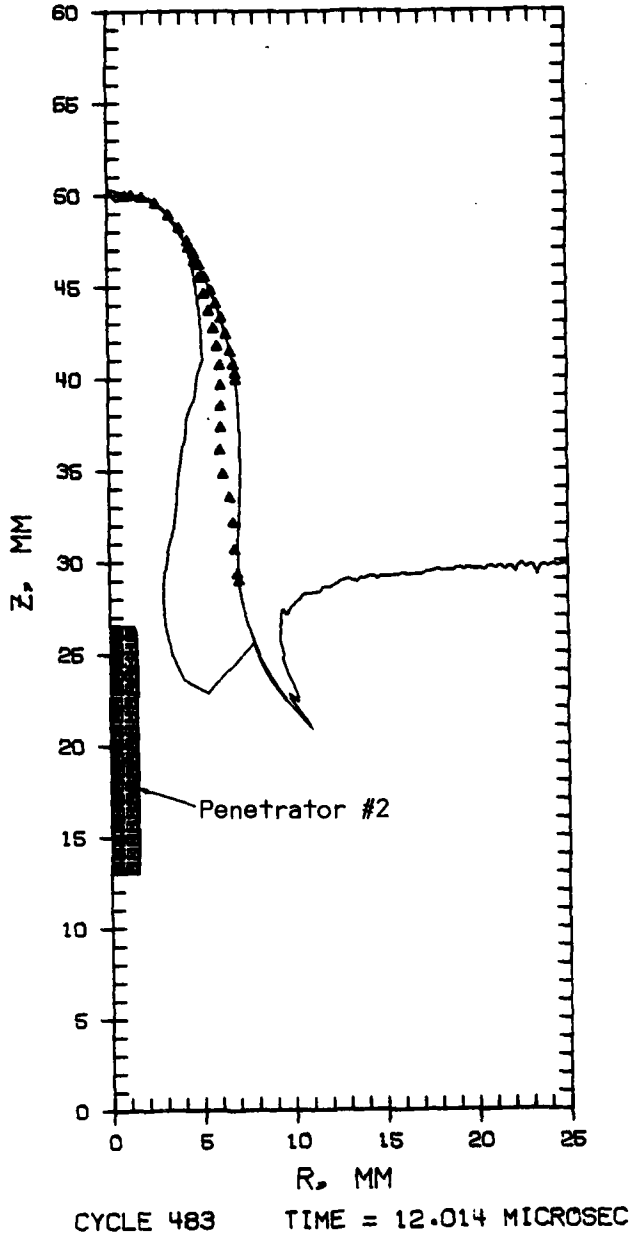

Figure 13. Double Impact Penetrator-Target Deformation for a 50-mm Penetrator Separation

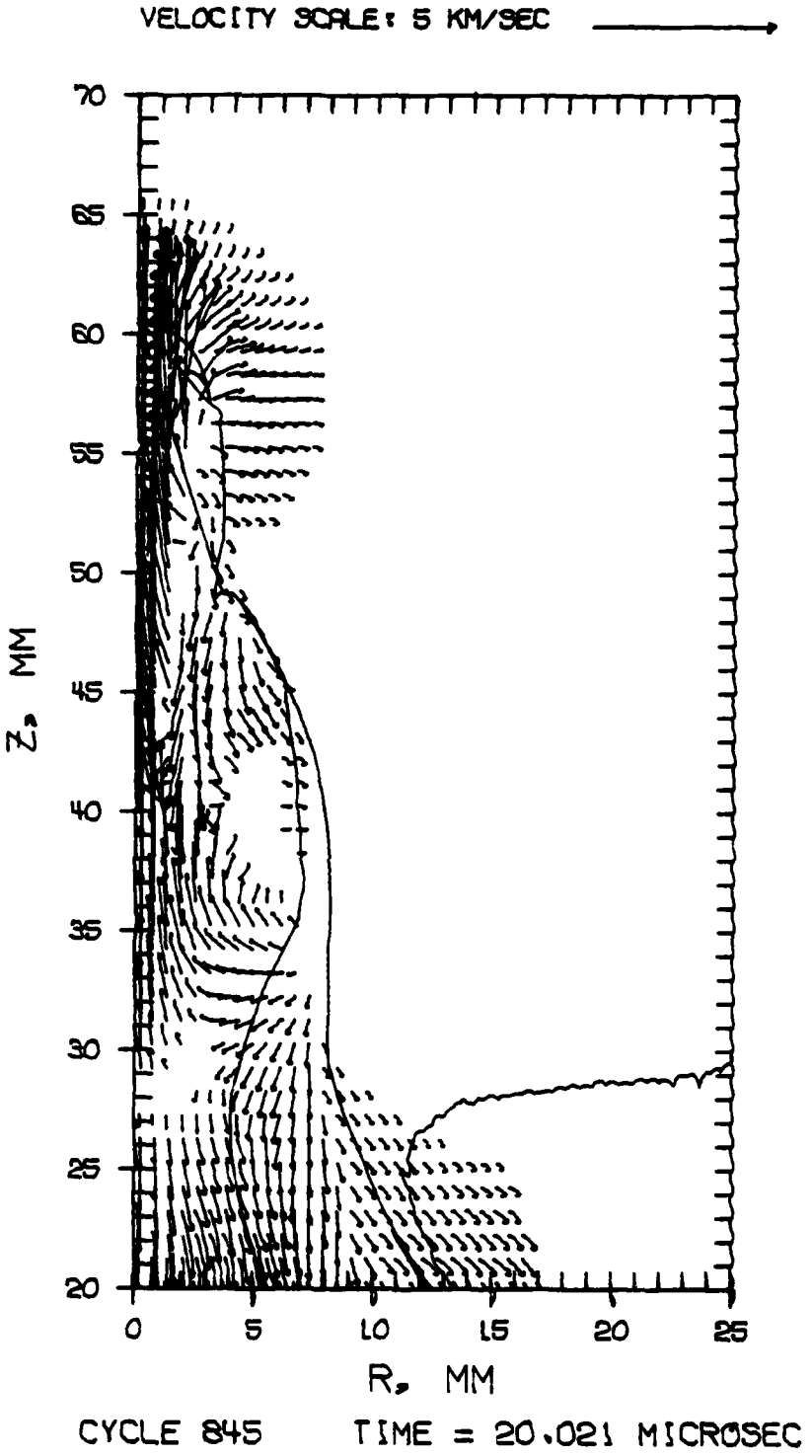

Figure 14. Double Impact Velocity Field for a 50-mm Penetrator Separation

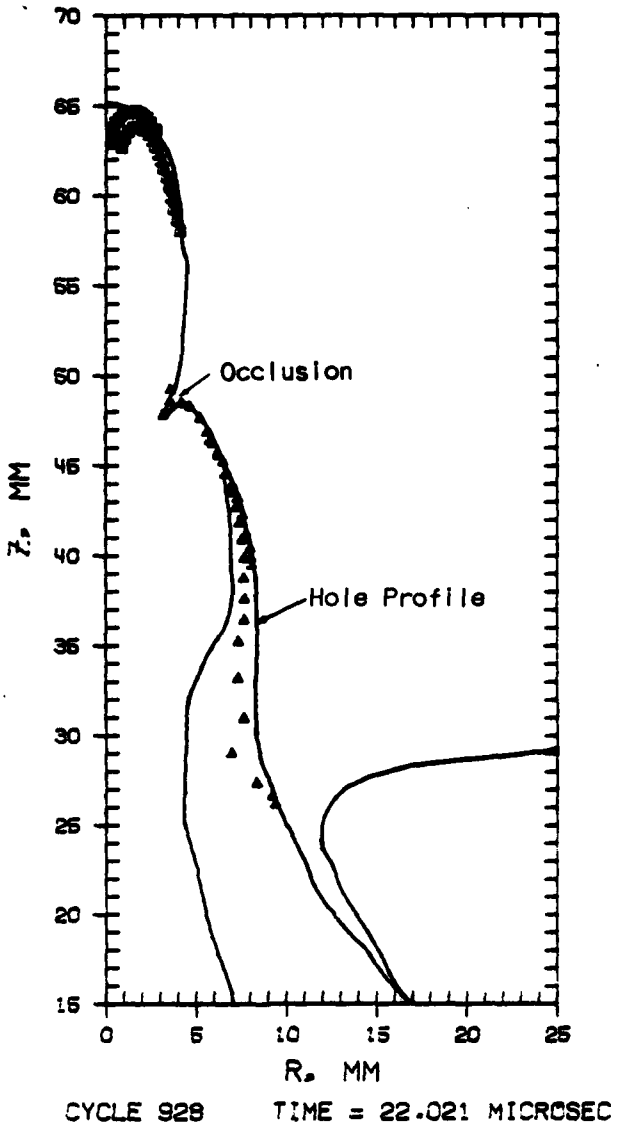

Figure 15. Double Impact Penetrator-Target Deformation for a 50-mm Penetrator Separation

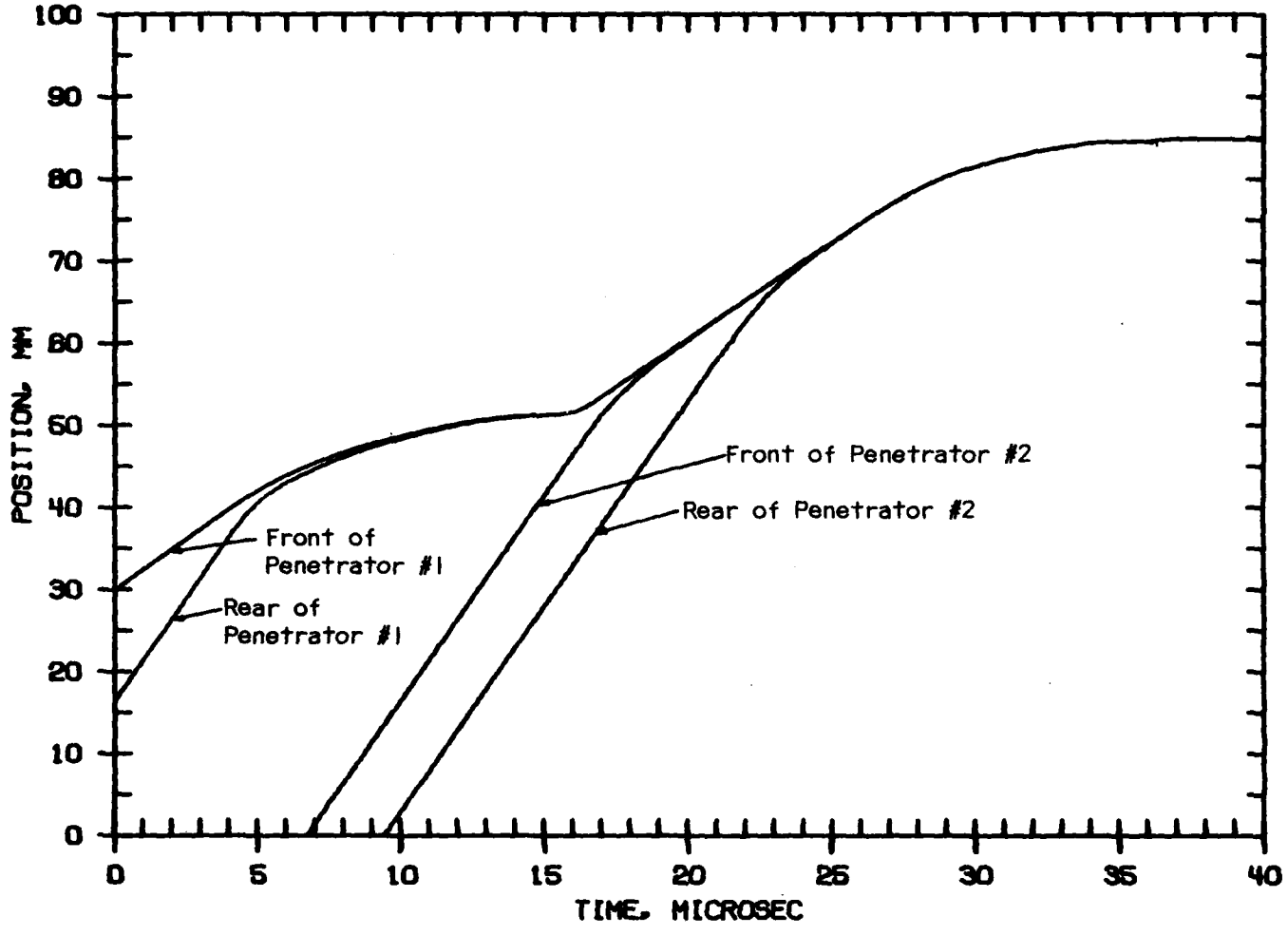

Figure 16. Double Impact Tracer Motion History for a 50-mm Penetrator Separation

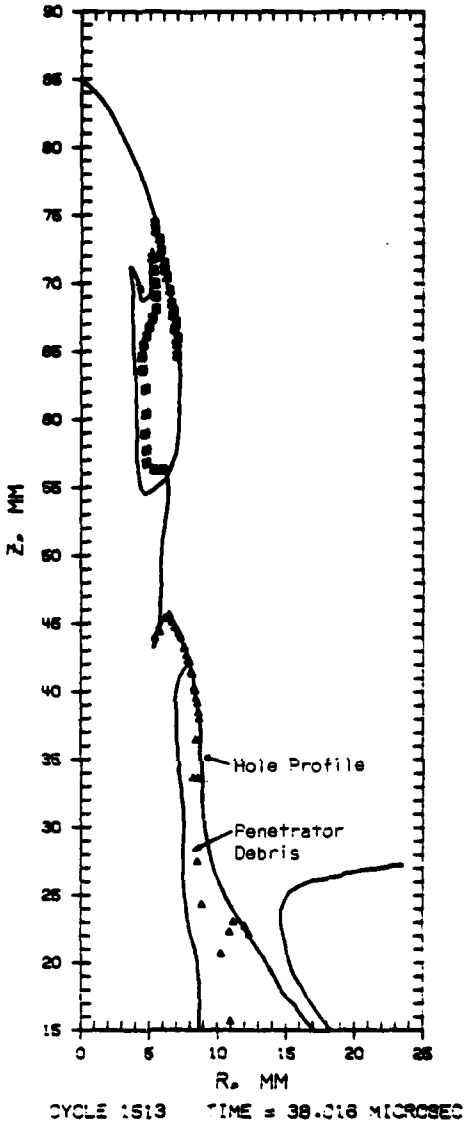

Figure 17. Double Impact Hole Profile for a 50-mm Penetrator Separation

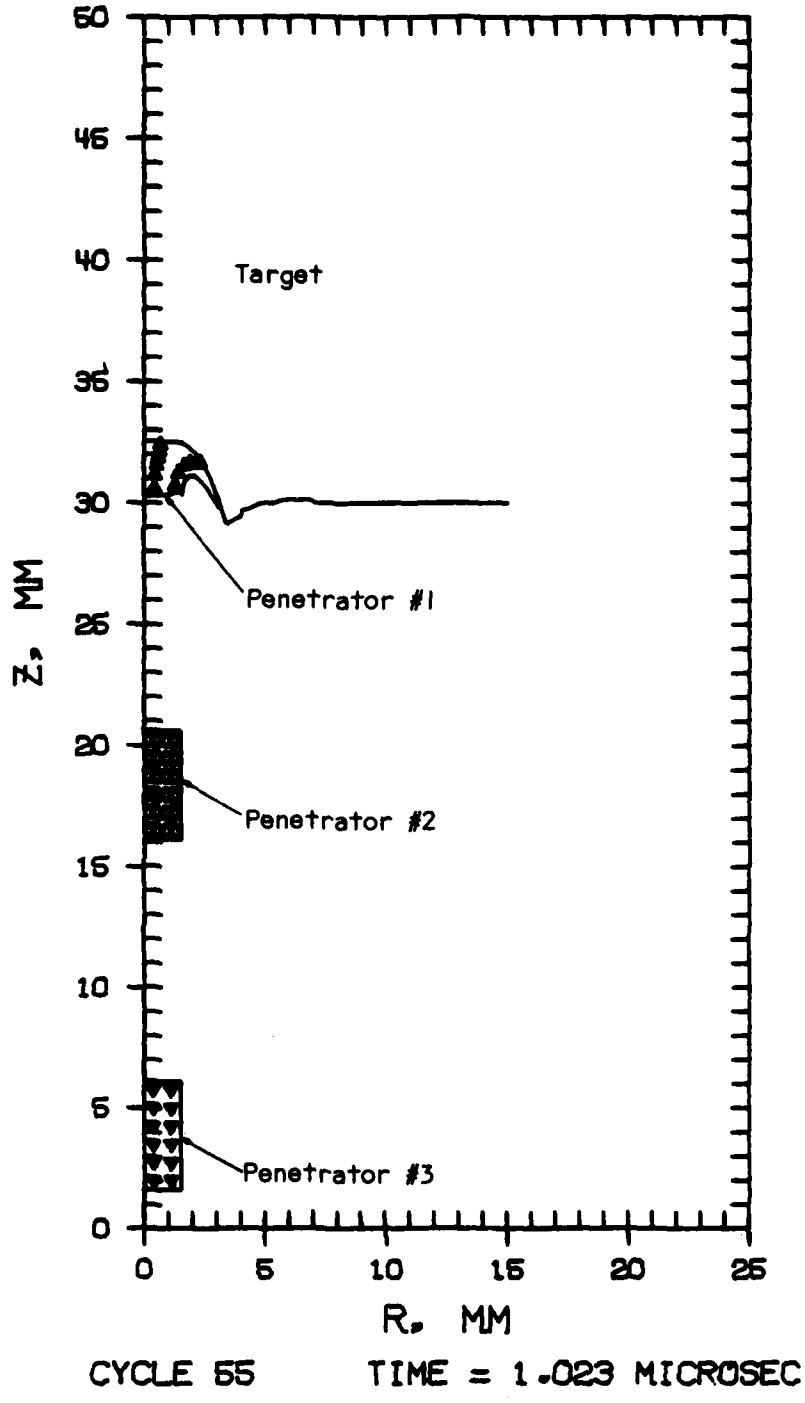

Figure 18. Sextuple Impact Penetrator-Target Deformation for a 10-mm Penetrator Separation

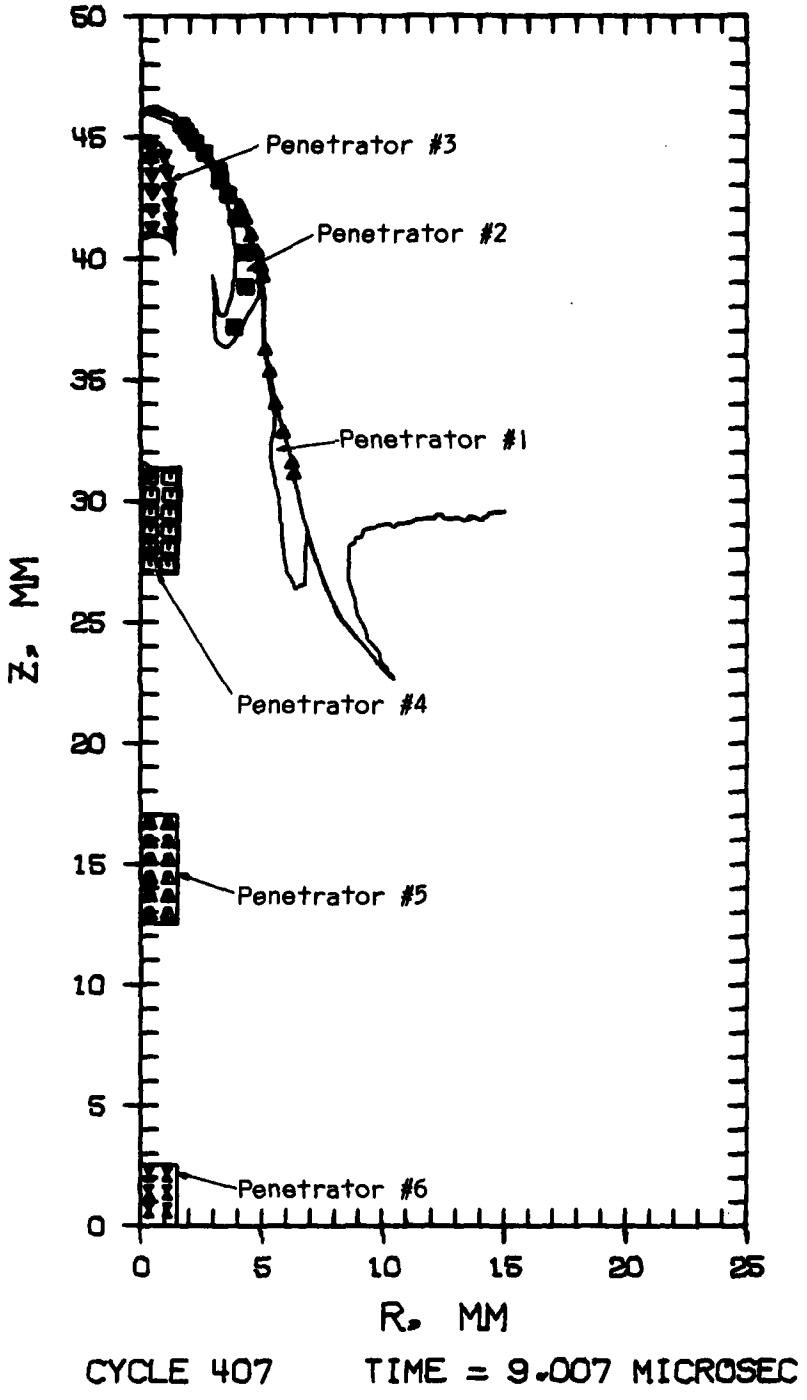

Figure 19. Sextuple Impact Penetrator-Target Deformation for a 10-mm Penetrator Separation

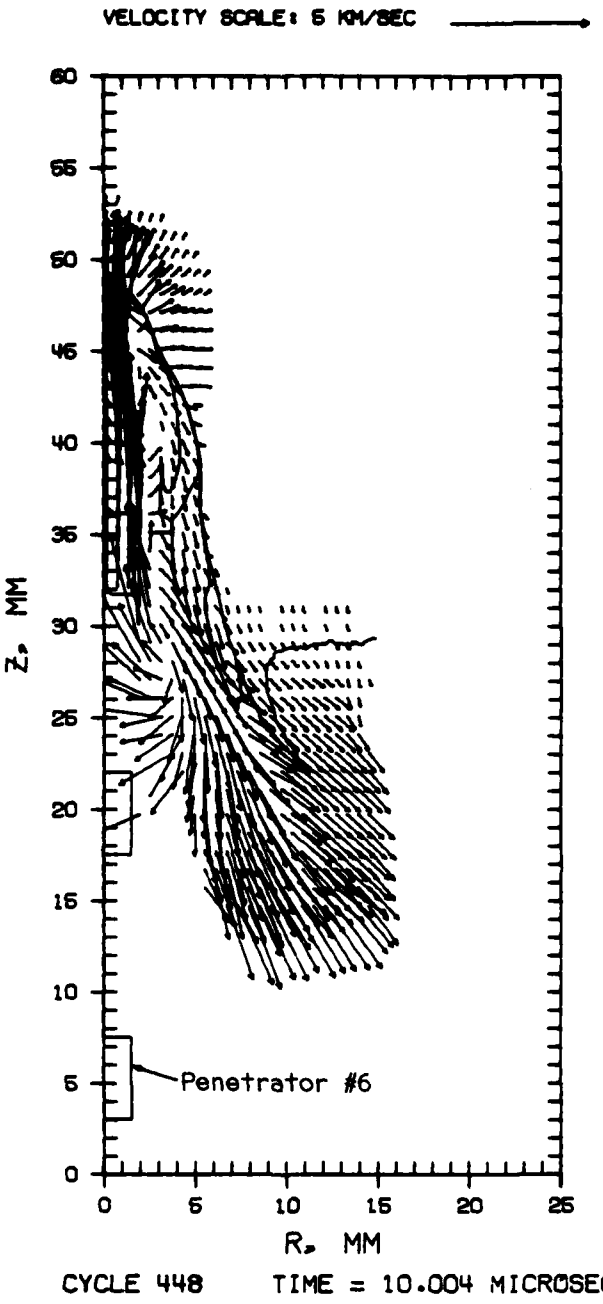

Figure 20. Sextuple Impact Velocity Field for a 10-mm Penetrator Separation

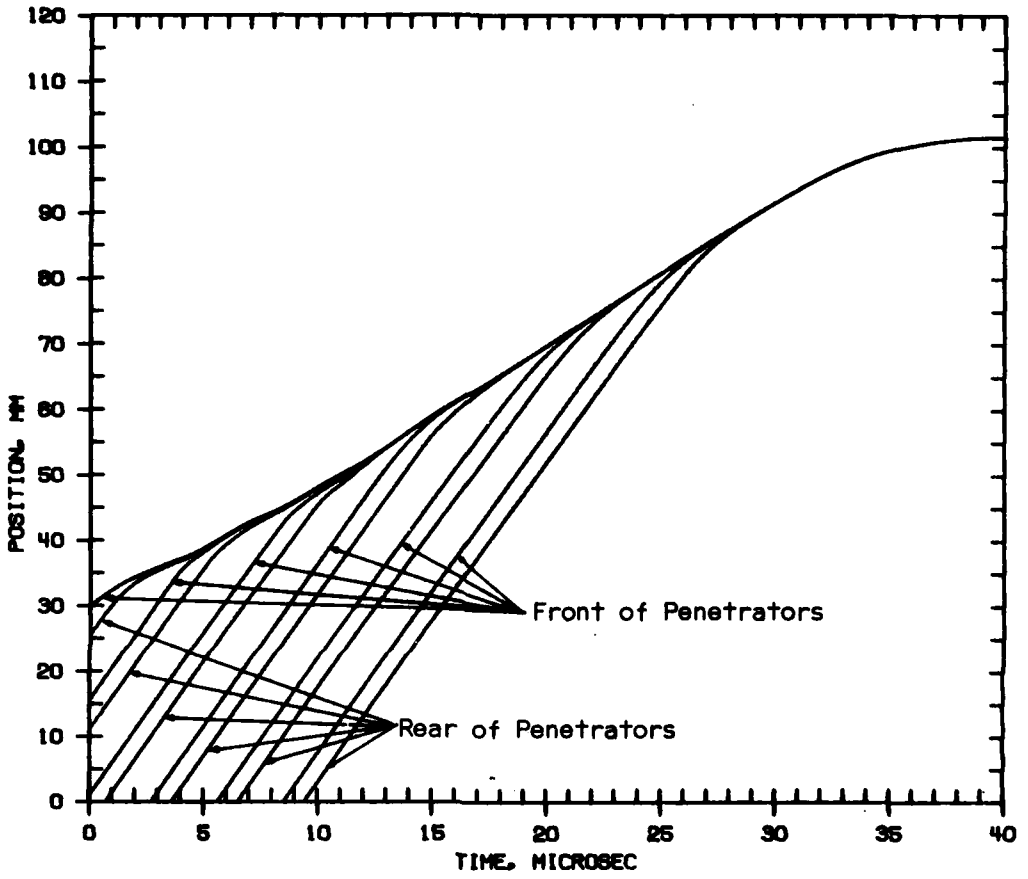

Figure 21. Sextuple Impact Tracer Motion History for a 10-mm Penetrator Separation

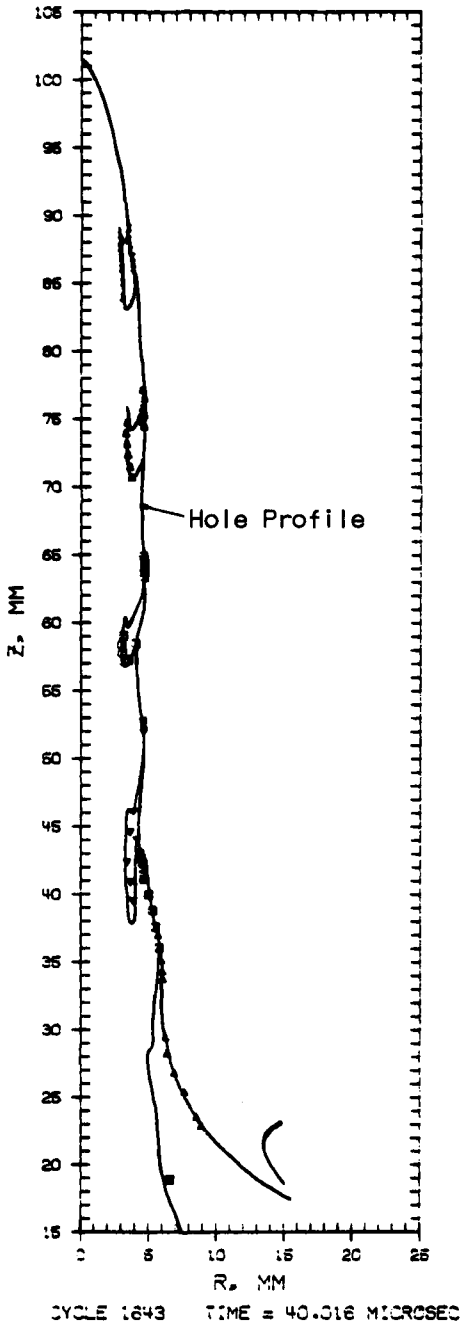

Figure 22. Sextuple Impact Hole Profile for a 10-mm Penetrator Separation

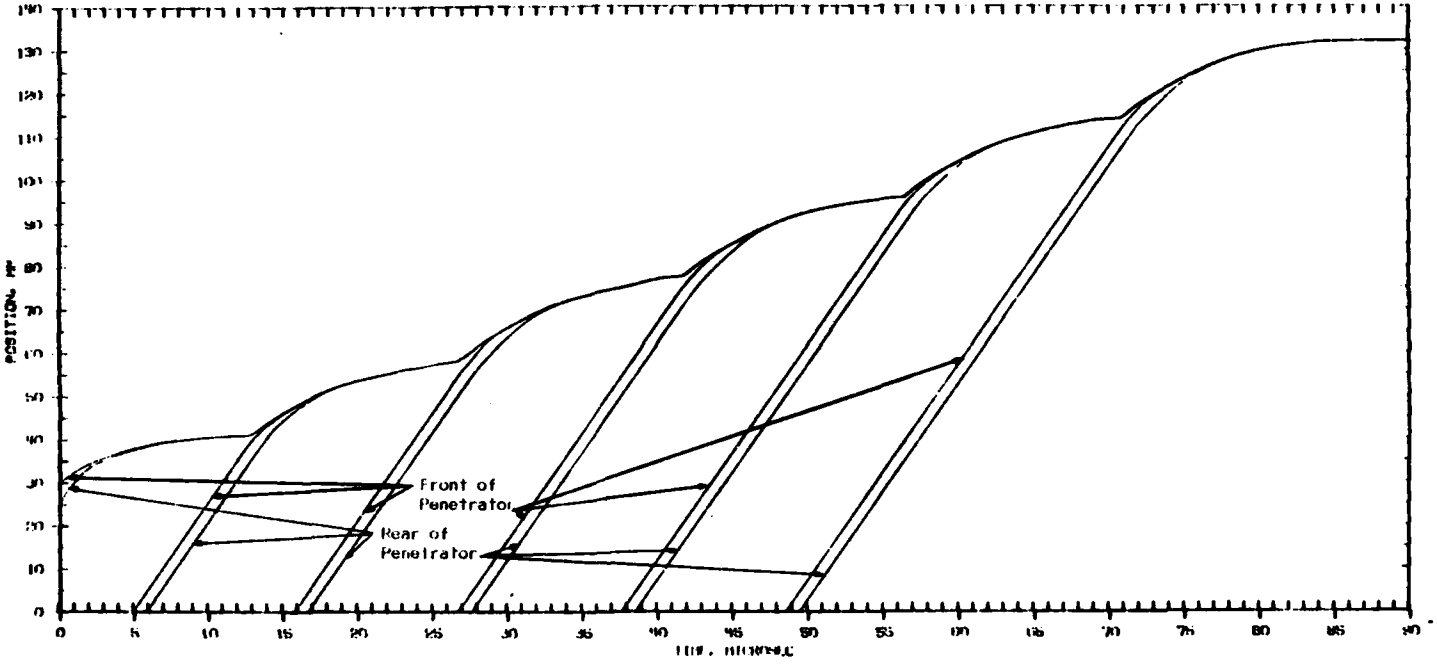

Figure 23. Sextuple Impact Tracer Motion History for a 50-mm Penetrator Separation

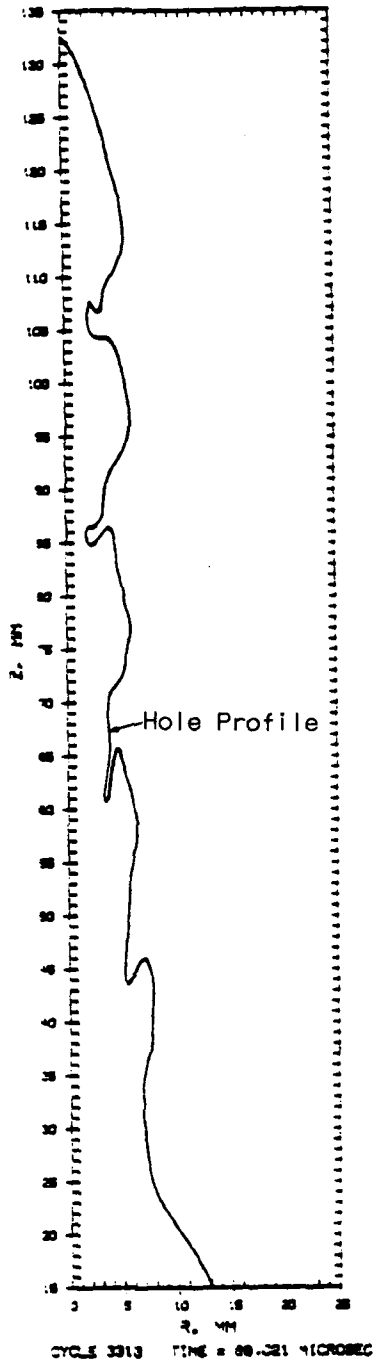

Figure 24. Sextuple Impact Hole Profile for a 50-mm Penetrator Separation

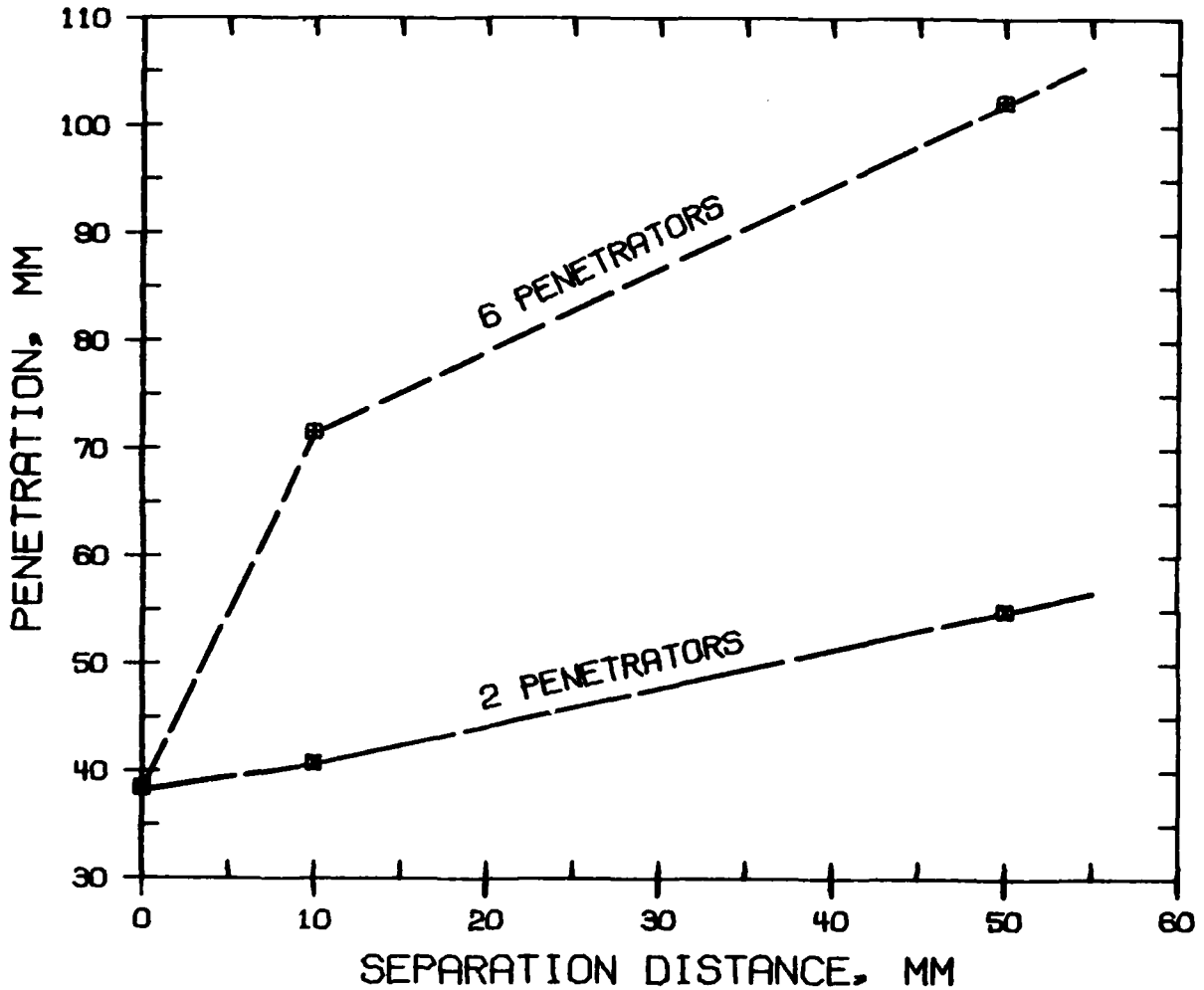

Figure 25. Relation Between the Penetrator Separation Distance, the Number of Penetrators, and the Maximum Penetration

REFERENCES

1. R. DiPersio, J. Simon, and A. Merendino, "Penetration of Shaped-Charge Jets into Metallic Targets," Ballistic Research Laboratory Report No. 1296, September 1965. (AD 476717)

2. A. Merendino and R. Vitali, "The Penetration of Shaped-Charge Jets into Steel and Aluminum Targets of Various Strengths," Ballistic Research Laboratory Memorandum Report No. 1932, August, 1968. (AD 392672)

3. W. P. Walters and J. N. Majerus, "Impact Models for Penetration and Hole Growth," BRL Technical Report ARBRL-TR-02069, May 1978. (AD A056294)

4. W. P. Walters and J. N. Majerus, "Shaped-Charge Penetration Model, Part 1: Monolithic Penetration and Comparison with Experimental Data," BRL Technical Report ARBRL-TR-02184, August 1979. (AD B041747L)

5. W. E. Johnson, "Development and Application of Computer Programs Related to Hypervelocity Impact," Systems, Science and Software, 3SR-749, July 1971. (AD 889143)

6. J. H. Tillotson, "Metallic Equations of State for Hypervelocity Impact," Gulf General Atomic, GA-3216, July 1962.

7. V. Kucher, "Preliminary Computer Computations for Slender Rod Impact Problems," Ballistic Research Laboratory Report No. 1957, February 1977. (AD A036995)

DISTRIBUTION LIST

No. of Copies	Organization
12	Commander Defense Technical Info Center ATTN: DTIC-DDA Cameron Station Alexandria, VA 22314
1	Commander US Army Materiel Development and Readiness Command ATTN: DRCDMD-ST 5001 Eisenhower Avenue Alexandria, VA 22333
2	Commander US Army Armament Research and Development Command ATTN: DRDAR-TSS (2 cys) Dover, NJ 07801
1	Commander US Army Armament Materiel Readiness Command ATTN: DRSAR-LEP-L, Tech Lib Rock Island, IL 61299
1	Director US Army ARRADCOM Benet Weapons Laboratory ATTN: DRDAR-LCB-TL Watervliet, NY 12189
1	Commander US Army Aviation Research and Development Command ATTN: DRDAV-E 2300 Goodfellow Blvd St. Louis, MO 63120
1	Director US Army Air Mobility Research and Development Laboratory Ames Research Center Moffett Field, CA 94035
1	Commander US Army Communications Rsch and Development Command ATTN: DRDCO-PPA-SA Fort Monmouth, NJ 07703
1	Commander US Army Electronics Research and Development Command Technical Support Activity ATTN: DELSD-L Fort Monmouth, NJ 07703
1	Commander US Army Missile Command ATTN: DRSMI-R Redstone Arsenal, AL 35898
1	Commander US Army Missile Command ATTN: DRSMI-YDL Redstone Arsenal, AL 35898
1	Commander US Army Tank Automotive Rsch and Development Command ATTN: DRDTA-UL Warren, MI 48090
1	Director US Army TRADOC Systems Analysis Activity ATTN: ATAA-SL, Tech Lib White Sands Missile Range, NM 88002
1	AFELM, The Rand Corporation ATTN: Library-D 1700 Main Street Santa Monica, CA 90406

DISTRIBUTION LIST

No. of Copies	Organization
2	Chief of Naval Research Department of the Navy ATTN: Code 427 Code 470 Washington, DC 20360
2	Commander US Naval Air Systems Command ATTN: Code AIR-310 Code AIR-350 Washington, DC 20360
1	Commander US Naval Research Laboratory Washington, DC 20375
1	Commander US Naval Surface Weapons Center ATTN: DX-21, Lib. Br. Dahlgreen, VA 22448
1	Commander US Naval Surface Weapons Center ATTN: Code 730, Lib Silver Spring, MD 20910
1	Commander US Naval Weapons Center ATTN: Code 45, Tech Lib China Lake, CA 93555
1	USAF (AFRDDA) Washington, DC 20330
1	AFSC (SDW) Andrews AFB Washington, DC 20331
1	US Air Force Academy ATTN: Code FJS-RL (NC) Tech Lib Colorado Springs, CO 80940
1	Ogden ALC/MMWRE (Mr. Ted E. Comins) Hill AFB, UT 84406
1	AFWL (SUL) Kirtland AFB, NM 87116
1	AFLC (MMWMC) Wright-Patterson AFB, OH 45433
1	AFAL (AVW) Wright-Patterson AFB, OH 45433
1	Director National Aeronautics and Space Administration Langley Research Center Langley Station Hampton, VA 23365
4	Director Lawrence Livermore Laboratory ATTN: Mr. M. Wilkins Dr. C. Godfrey Dr. G. Goudreau Dr. R. Werne P. O. Box 808 Livermore, CA 94550
1	Computer Code Consultants, Inc. ATTN: Mr. W. Johnson 1680 Camino Redondo Los Alamos, NM 87544
1	Physics International Corp ATTN: Mr. L. Behrmann 2700 Merced Street San Leandro, CA 94577

DISTRIBUTION LIST

No. of Copies	Organization
1	Sandia Laboratories ATTN: Dr. L. Bertholf Albuquerque, NM 87115
1	Systems, Science and Software ATTN: Dr. R. Sedgwick P. O. Box 1620 La Jolla, CA 92037
3	Honeywell, Inc. Government and Aerospace Products Division ATTN: Mr. J. Blackburn Dr. G. Johnson Mr. R. Simpson 600 Second Street, NE Hopkins, MN 55343
1	Shock Hydrodynamics ATTN: Dr. L. Zernow 4710 Vineland Avenue North Hollywood, CA 91602
1	Southwest Research Institute Dept of Mechanical Sciences ATTN: Mr. A. Wenzel 8500 Culebra Road San Antonio, TX 78228
1	Drexel Institute of Technology Wave Propagation Research Center ATTN: Prof. P. Chou 32nd & Chestnut Streets Philadelphia, PA 19104
2	University of California Los Alamos Scientific Lab ATTN: Dr. J. M. Walsh Tech Lib P. O. Box 1663 Los Alamos, NM 87545

Aberdeen Proving Ground

Dir, USAMSAA
ATTN: DRXSY-D
DRXSY-MP, H. Cohen

Cdr, USATECOM
ATTN: DRSTE-TO-F

Dir, USACSL, Bldg. E3516, EA
ATTN: DRDAR-CLB-PA

USER EVALUATION OF REPORT

Please take a few minutes to answer the questions below; tear out this sheet, fold as indicated, staple or tape closed, and place in the mail. Your comments will provide us with information for improving future reports.

1. BRL Report Number _____

2. Does this report satisfy a need? (Comment on purpose, related project, or other area of interest for which report will be used.)

_____

_____

_____

3. How, specifically, is the report being used? (Information source, design data or procedure, management procedure, source of ideas, etc.) _____

_____

_____

4. Has the information in this report led to any quantitative savings as far as man-hours/contract dollars saved, operating costs avoided, efficiencies achieved, etc.? If so, please elaborate.

_____

_____

5. General Comments (Indicate what you think should be changed to make this report and future reports of this type more responsive to your needs, more usable, improve readability, etc.) _____

_____

_____

_____

6. If you would like to be contacted by the personnel who prepared this report to raise specific questions or discuss the topic, please fill in the following information.

Name: _____

Telephone Number: _____

Organization Address: _____

_____

_____